Talanta 99 (2012) 959–965

Contents lists available at SciVerse ScienceDirect

Talanta

journal homepage: www.elsevier.com/locate/talanta

Molecularly imprinted polymers based on multi-walled carbon nanotubes for selective solid-phase extraction of oleanolic acid from the roots of kiwi fruit samples

Xing Chen [a,b], Zhaohui Zhang [a,b,*], Xiao Yang [b], Jiaxing Li [b], Yunan Liu [b], Hongjun Chen [b], Wei Rao [b], Shouzhuo Yao [c]

[a] Key Laboratory of Hunan Forest Products and Chemical Industry Engineering, Jishou University, Zhangjiajie 427000, China
[b] College of Chemistry and Chemical Engineering, Jishou University, Jishou 416000, China
[c] State Key Laboratory of Chemo/Biosensing and Chemometrics, Hunan University, Changsha 410082, China

ARTICLE INFO

Article history:
Received 14 May 2012
Received in revised form
23 July 2012
Accepted 25 July 2012
Available online 2 August 2012

Keywords:
Surface molecular imprinting
Oleanolic acid
Multi-walled carbon nanotubes
High-performance liquid chromatography

ABSTRACT

This study describes the synthesis of novel molecularly imprinted polymers based on multi-walled carbon nanotubes (MWNTs@MIPs) using oleanolic acid as the template, 4-vinylpyridine as the functional monomer and divinylbenzene as the cross-linker by heat-induced polymerization. The MWNTs@MIPs were characterized with Fourier transform infrared (FT-IR) spectrometry and scanning electron microscopy (SEM). The adsorption process of the MWNTs@MIPs towards oleanolic acid was investigated in detail. The properties of MWNTs@MIPs for solid-phase extraction (SPE) were also evaluated. The results demonstrated the good imprinting effect and the comparable selectivity of MWNTs@MIPs. The optimized molecularly imprinted solid-phase extraction (MISPE) procedure was applied to extract oleanolic acid from the extracts of the roots of kiwi fruit samples. The recoveries of spiked oleanolic acid in kiwi fruit samples were in the range of 84–92.6% with relative standard deviations below 5%, and its limit of detection reached 2.56 $\mu g\,L^{-1}$.

1. Introduction

Oleanolic acid, an important triterpene, which is present in more than 120 plant species, possesses many important biological activities, such as antitumor, hepatoprotective and hypolipidemic effects[1,2]. At present, oleanolic acid is obtained mainly from plant extracts due to its complicate structure, which is difficult to synthesize [3]. The plant extracts were obtained from plant tissue by several conventional methods, such as maceration extraction, reflux and soxhlet extraction, of which are solvent- and time-consuming [4]. Thus, developing an efficient separation and pre-concentration technology for oleanolic acid is extremely important.

Generally, liquid–liquid extraction (LLE) and solid-phase extraction (SPE) are commonly used for pre-concentration and clean-up in the analysis of biological and environmental samples. However, the time consuming and needing large amount of solvent of LLE resulted in the complicated pretreatment and the pollution of the environment [5]. SPE is widely used due to the advantages of simplicity, rapidness and less consumption of organic solvents. Furthermore, it is easy to couple with gas chromatography (GC) or high-performance liquid chromatography (HPLC) [6]. The SPE consists of the separation and concentration of the analyte from a complex sample by adsorption onto an appropriate sorbent, removal of interfering impurities by washing with a suitable solvent system, and selective recovery of the retained analyte with a fitted solvent [7]. However, the low selectivity is a harder problem for common SPE sorbents when an extraction for complex matrix has to be performed. Fortunately, this separation and concentration can potentially be realized by using molecularly imprinted polymers (MIPs) to bind the target molecule in a selective manner, even when the analyte is present in complex matrix. The first combination of MIPs and SPE was reported by Sellergren [8]. Essentially, molecular imprinting is a state-of-the-art technique for the preparation of tailor-made receptors which can selectively bind predetermined target molecules. In other words, recognition sites were generated

Abbreviations: AIBN, 2,2-azobisisobutyronitrile; CNTs, carbon nanotubes; FT-IR, Fourier transform infrared spectrometry; MIPs, molecularly imprinted polymers; MWNTs, multi-walled carbon nanotubes; TC, thionylchloride; 4-VP, 4-vinylpyridine; DVB, divinylbenzene; TETA, triethylenetetraamine; DMF, *N*,*N*-dimethylformamide; THF, tetrahydrofuran; MWNTs-R-NH_2, MWNTs-$CONH(CH_2CH_2NH)_2$ $CH_2CH_2NH_2$; MISPE, molecularly imprinted solid-phase extraction; NISPE, non-imprinted solid-phase extraction

* Corresponding author at: College of Chemistry and Chemical Engineering, Jishou University, Jishou 416000, China. Tel.: +86 743 8563911; fax: +86 743 8563911.
E-mail address: zhaohuizhang77@163.com (Z. Zhang).

0039-9140/$ - see front matter © 2012 Elsevier B.V. All rights reserved.
http://dx.doi.org/10.1016/j.talanta.2012.07.066

by polymerizing functional monomer together with the template molecules in the presence of a cross-linking agent. After removing of the template molecules, imprinted cavities which were complementary in shape, size and functional groups to the template molecules were left inside the polymer network [9]. These artificial receptors have been proved useful in various applications based on molecular recognition [10–13]. However, MIPs which were prepared by traditionally bulk polymerization exhibited highly selective recognition but with poor accessibility to the template, as the template molecules were embedded inside the thick polymer network. In order to overcome this drawback, surface molecular imprinting method that attempts to build molecular recognition systems on the support materials surface with nanoscale dimensions was introduced, where the template molecules could be assembled on the surface of such support materials. The support materials consist of clay platelets [14], polypropylene fiber [15], inorganic nanoparticles [16–18] and graphene [19]. Among these materials, multi-walled carbon nanotubes (MWNTs) have been proved to be an available support material in surface imprinting process [20]. It is well known that MWNTs possess extraordinarily high aspect ratios and unique atomic structures [21], these properties reveal that they can be used for preparing reinforced polymer composites.

In this paper, oleanolic acid-imprinted polymers coated on MWNTs (MWNTs@MIPs) surface were synthesized with 4-vinylpyridine as the functional monomer and divinylbenzene as the cross-linker. The molecular recognition performance of oleanolic acid-imprinted polymers was investigated in detail. Moreover, the MWNTs@MIPs were successfully applied as selective SPE materials coupled with HPLC to enrich oleanolic acid from kiwi fruit samples.

2. Experimental

2.1. Chemicals and reagents

Multi-walled carbon nanotubes with diameter of 30–50 nm and length of 20 μm (MWNTs, purity >95 wt%) were supplied by Shenzhen Bill Corporation. Oleanolic acid, ursolic acid, rhein and emodin, whose chemical structures are shown in Fig. 1, were purchased from Shanxi Xuhuang Botanical Science and Technology Development Company (Xi'an, China). 4-Vinylpyridine (4-VP) was obtained from Merck (Germany) and distilled under vacuum before use and kept at $-4\,^{\circ}C$ in the dark. Divinylbenzene (DVB) was purchased from Sigma (USA). 2, 2′-Azobis-isobutyronitrile (AIBN), triethylenetetraamine (TETA), thionylchloride (TC), *N, N*-dimethylformamide (DMF), tetrahydrofuran (THF), chloroform, acetonitrile, acetic acid, nitric acid and methanol were purchased from Changsha Chemical Reagent Company (Hunan, China). All the chemicals used were analytical reagent grade. Ultrapure water was employed throughout the experiment.

2.2. Pretreatment of multi-walled carbon nanotubes

The amine groups were introduced on the surface of MWNTs in the following steps. Firstly, 0.5 g of raw MWNTs was initially dispersed into 50 mL of nitric acid (65 wt%) under 80 °C heating for 24 h. Then cooled to the room temperature, the acid treated MWNTs were diluted in water, filtered, washed with ultrapure water and dried in vacuum at 40 °C overnight. Thus the acid-oxidation MWNTs (MWNTs-COOH) were obtained. Next step, the MWNTs-COOH were converted to acid chloride-functionalized (MWNTs-COCl) by reacting with TC at 80 °C for 24 h. The residual TC was removed by distillation. Subsequently, 6.2 g of TETA and 70 mL of DMF were added under vigorous magnetic stirring and then reacted at 80 °C for 24 h to obtain amine group functionalized MWNTs (MWNTs-CONH($CH_2CH_2NH)_2CH_2CH_2NH_2$, abbreviated as MWNTs-R-NH_2).

2.3. Preparation of MWNTs@MIPs

MWNTs-R-NH_2 (200 mg), oleanolic acid (0.5 mmol, 0.2284 g), 4-VP (2 mmol, 0.2103 g) and 50 mL of DMF were blended under sonication for 0.5 h to obtain the prepolymerization mixture. Then DVB (10 mmol, 1.301 g), AIBN (0.36 mmol, 60 mg) and 50 mL of DMF were sonicated evenly for 0.5 h, and transferred into the previous pre-polymerization mixture. To degas this solution, nitrogen was purged for 0.5 h. Next, the flask was sealed and left polymerizing at 60 °C in a water bath under nitrogen protection. The polymers were washed successively with methanol/acetic acid (9:1; v/v) until no oleanolic acid molecule was

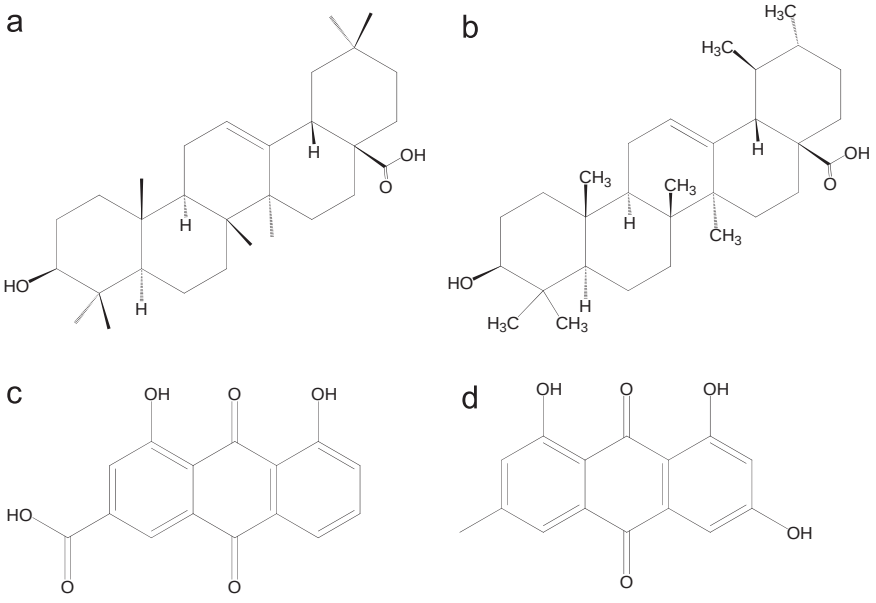

Fig. 1. Chemical structures of oleanolic acid (a), ursolic acid (b), rhein (c), and emodin (d).

detected in the effluent by a UV–vis spectrometer (UV-2450, SHIMADZU, Japan) at 210 nm. Eluted with ultrapure water, the polymers were dried overnight under vacuum at 60 °C. The non-imprinted polymers based on multi-walled carbon nanotubes (MWNTs@NIPs) were prepared identically to the imprinted polymers but omitting the template oleanolic acid.

2.4. Characterization

The infrared spectra of MWNTs, MWNTs-R-NH_2 and MWNTs@MIPs were recorded on a Nicolet Magna-560 Fourier transform infrared (FT-IR) spectrometer. The morphologies of MWNTs and MWNTs@MIPs were examined by a scanning electron microscopy (SEM, JSM-6700F).

High-performance liquid chromatography (HPLC) analysis was conducted with a LC-2010AHT solution system (SHIMADZU, Japan) and a UV–vis detector which was set at 210 nm. Analytical separations were achieved on a Spherigel C_{18} column (5 μm, 150 mm × 4.6 mm). The mobile phase of the HPLC experiment was composed of acetonitrile and ultrapure water (90:10; v/v), which was filtered through 0.45 μm polytetrafluoroethylene (PTFE) membranes before use.

2.5. Adsorption experiment

Ten milligrams of MWNTs@MIPs or MWNTs@NIPs were added into 10 mL of oleanolic acid solutions with different concentrations from 10 to 100 mg L^{-1} for 120 min at room temperature. After static adsorption, the polymers were separated by centrifugation and oleanolic acid concentration in the supernatant was measured by UV–vis spectrometry at 210 nm.

A series of oleanolic acid standard solutions were prepared for calibration curve. Adsorption capacity Q (mg g^{-1}) was calculated from Eq. (1) [22]

$$Q = (C_i - C_f) \times V/m \quad (1)$$

where C_i (mg L^{-1}) and C_f (mg L^{-1}) are the initial and final concentrations of oleanolic acid, respectively, V (L) is the volume of the solution, m (g) is the weight of MWNTs-MIPs or MWNTs-NIPs.

The kinetic adsorption test was performed by changing the adsorption time from 0 to 120 min while keeping oleanolic acid initial concentration of 50 mg L^{-1}. The saturated adsorption capacity was obtained based on Langmuir adsorption Eq. (2) [22]

$$Q = KC_eQ_{max}/(1 + KC_e) \quad (2)$$

where Q (mg g^{-1}) and Q_{max} (mg g^{-1}) are the equilibrium adsorbed amount and theoretical maximum adsorption capacity of oleanolic acid, respectively, C_e (mg L^{-1}) is the concentration of oleanolic acid in equilibrium solution, K (L mg^{-1}) is the Langmuir adsorption equilibrium constant towards oleanolic acid.

2.6. Selectivity experiment

To measure the selective recognition of the imprinted polymers towards oleanolic acid, the competitive adsorption experiments toward ursolic acid, rhein and emodin were performed. During the experiment, 10 mL of 50 mg L^{-1} coexisting compounds (oleanolic acid, ursolic acid, rhein and emodin) solution was treated according to the procedure of adsorption studies in Section 2.5. The effect of imprinting on selectivity was defined [23] as follows:

$$K_d = (C_i - C_f)V/mC_f \quad (3)$$

where K_d (L g^{-1}) is the distribution coefficient, C_i (mg L^{-1}) and C_f (mg L^{-1}) are the initial and final solution concentrations, respectively, V (L) is the volume of solution used for the extraction and m (g) is the weight of polymer used for extraction.

The selectivity coefficient (k) for the binding of oleanolic acid in the presence of competitive compounds can be obtained from equilibrium binding data according to Eq. (4)

$$k = K_{\text{template}}/K_{\text{competing compounds}} \quad (4)$$

The relative selectivity coefficient was defined as follows:

$$k' = K_{\text{imprinted}}/K_{\text{non-imprinted}} \quad (5)$$

2.7. Optimization of SPE

MWNTs@MIPs (100 mg) or MWNTs@NIPs (100 mg) were packed respectively into an empty stainless steel SPE column (150 mm × 4.6 mm, i.d.). The polypropylene upper and lower frits remained at each end of the column to hold the packing in place. Before loading sample solutions, the column should be activated through 10 mL of methanol at a flow rate of 1.0 mL min^{-1}. The activated molecularly imprinted SPE (MISPE) columns were washed with 10 mL of pure water to remove the impurities firstly. To optimize the MISPE procedures, the loading, washing and elution solvent were investigated. In the loading process, oleanolic acid dissolved in the solvent of THF, DMF and methanol (10 mL, 50 mg L^{-1}) was passed through the imprinted or non-imprinted polymer column, respectively. In the next procedure, the column was washed respectively with chloroform, acetonitrile, and methanol (3 mL) to reduce non-specific adsorption. Afterward, the extracted oleanolic acid was striped from the column using methanol containing 1–20% acetic acid solutions. Each elution fraction was then collected in a centrifuge tube and concentrated to dryness under nitrogen and re-dissolved with 10 mL of mobile phase of HPLC. Finally, the concentration of oleanolic acid was determined by HPLC.

The recovery percentage of oleanolic acid after loading, washing and eluting were calculated according to the formula (6)

$$\text{Recovery percentage} = C_t/C \times 100\% \quad (6)$$

where C (mg L^{-1}) is the initial concentration of oleanolic acid before loading and C_t (mg L^{-1}) is the concentration of oleanolic acid eluted from the MISPE column after loading, washing and eluting, respectively.

2.8. MISPE procedure for the determination of oleanolic acid in real samples

The roots of kiwi fruit samples (1.0 g) collected in the nature were immersed by 100 mL of methanol in a 250 mL vessel and sonicated for 30 min. After the samples were extracted for 2 h at 80 °C, the extracts were filtered through a 0.45 μm PTFE membrane. To assess the accuracy and precision, real samples spiked with oleanolic acid, ursolic acid, rhein and emodin each at three different levels of 1.0, 2.0 and 3.0 mg L^{-1} were investigated (n=3). Finally, the extract was determined under the optimized SPE conditions coupled with HPLC.

3. Results and discussions

3.1. Synthesis of the MWNTs@MIPs

The synthetic route of MIPs based on MWNTs was shown in Fig. 2. Firstly, the amino-functionalized group was introduced stepwisely on the surface of the MWNTs. Next, the prepolymerization was done by mixing the functional monomer with the

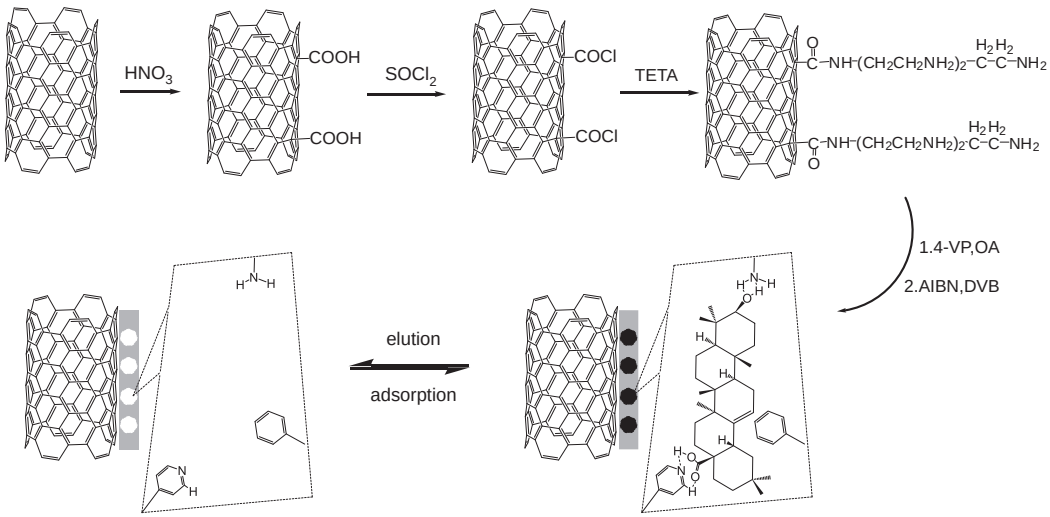

Fig. 2. The protocol for synthesis of MWNTs@MIPs.

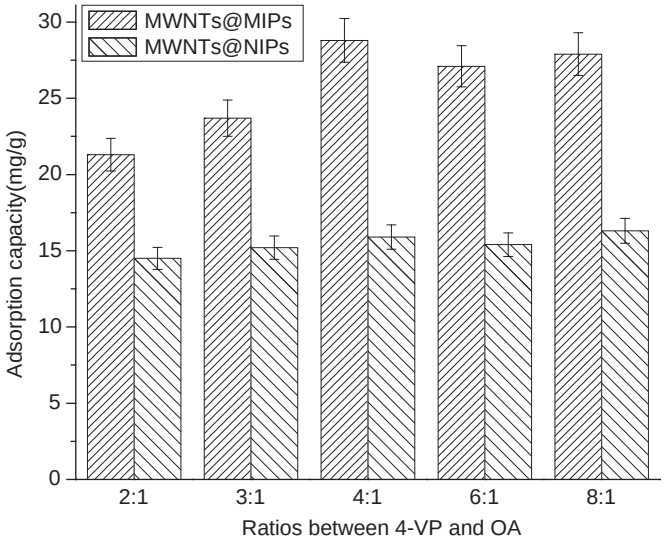

Fig. 3. Evaluation on the adsorption of MWNTs@MIPs composited of various ratios between 4-VP and oleanolic acid.

template oleanolic acid and amino-functionalized MWNTs. In this process, the functional monomer interacted with the template most intensively to give the complex high stability through non-covalent bonds [24], which facilitated the subsequent polymerization and the formation of the imprinted cavities with complementary structure to the template on the surface of MWNTs. After the template molecules were removed, a large number of tailor-made cavities for the template on the surface of MWNTs was formed. As shown in Fig. 1, oleanolic acid has two functional groups involving carboxylic acid and hydroxyl, which are susceptible to interact with functional monomers. To form stable host-guest complexes between the template oleanolic acid and functional monomers, alkaline monomer 4-VP was chosen as the functional monomer [25]. Except for crosslinking, the copolymerization of DVB could also enable the production of dispersion [26]. Generally, proper molar ratio of the functional monomer to the template is crucial to increase the specific recognition ability of the imprinted polymers and the number of imprinted cavities. The molar ratios of 4-VP to the template oleanolic acid were investigated as following studies. Five kinds of molar ratios between 4-VP and oleanolic acid of 2:1, 3:1, 4:1, 6:1 and 8:1 were investigated in this experiment. As shown in Fig. 3, the optimum ratio of the functional monomer to the template for the specific rebinding of oleanolic acid was 4:1, which exhibited the best specific affinity and the highest adsorption quantity of 28.8 mg g^{-1}, while that of the corresponding NIPs was 15.9 mg g^{-1}. However, when the ratio of the functional monomer to the template was greater or lower than 4:1, the binding capacities of MIPs toward oleanolic acid decreased, which can be attributed that the excessive functional monomer in high ratios of the functional monomer to the template is susceptible to form non-specific sites, while low ratios to produce fewer complexation because of insufficient functional groups [25, 27].

3.2. Characterization

The FT-IR spectra of MWNTs, MWNTs-R-NH_2 and MWNTs@MIPs were recorded in the range of 500–4000 cm^{-1} by KBr pellet method and the results were exhibited in Fig. S1 (shown in Supplementary Material). The MWNTs-R-NH_2 displayed the characteristic bands of primary (NH_2) and secondary amide (N–H) at 3500 and 3358 cm^{-1}, respectively. The bands at 1666, 1579, 1365 and 557 cm^{-1} (shown in Fig. S1b) were due to the presence of CONH on the surface of MWNTs-R-NH_2, and the bands at 1190 and 1213 cm^{-1} were attributed to the C–N stretching, the other bands at 1306 and 1082 cm^{-1} associated with the mixed C–N stretching and N–H bending vibrations of the acyl group. As shown in Fig. S1c, the band 712 cm^{-1} was assigned for 4-monosubstituted pyridine. And the bands at 1666 cm^{-1} and doublet bands at 1385 and 1521cm^{-1} were due to the stretching of C–N and C–C of 4-VP. These results confirmed successful polymerization of 4-VP. Furthermore, the bands at 1618, 788 and 894 cm^{-1} were attributed for disubstituted benzenoid rings and 1, 3-disubstituted C–H wagging of the cross-linkers DVB. Based on the above results, it can be concluded that the polymerization procedure was performed successfully.

Scanning electron microscopy (SEM) was employed to capture the detailed morphology of the MWNTs and MWNTs@MIPs. As shown in Fig. 4, the pristine MWNTs were in the form of individual tube with the diameter of 30–50 nm. And the diameters of the MWNTs@MIPs were about 160–200 nm. Thus, the average thickness of MIPs layer modified on the MWNTs could be calculated as 65–80 nm. Compared with the pristine MWNTs, the MWNTs@MIPs exhibited a slightly rough surface, which may assist oleanolic acid to be rebinded rapidly.

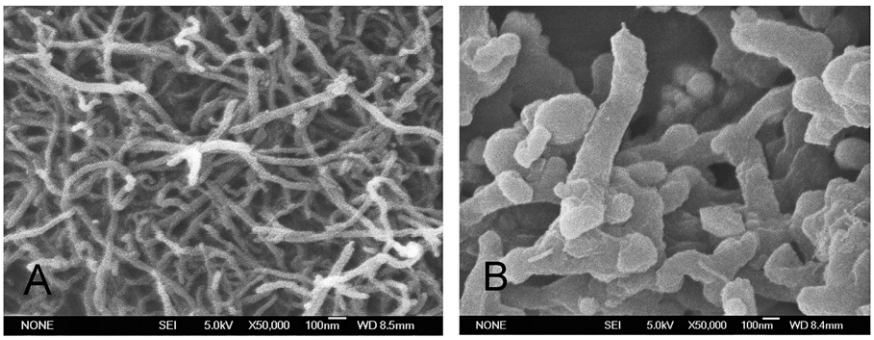

Fig. 4. Scanning electron micrographs of crude MWNTs (a) and MWNTs@MIPs (b).

3.3. Recognition properties of the MWNTs@MIPs

The binding properties of MWNTs@MIPs or MWNTs@NIPs at different time and various initial concentrations of oleanolic acid were evaluated and the results were shown in Supplementary Material Fig. S2. The MWNTs@MIPs reached adsorption equilibrium at 60 min and the adsorption process before equilibrium can be divided into two steps: rapid increases with the time increasing within the first 30 min and then levels off as equilibrium reached. It could be also observed that the MWNTs@MIPs exhibited a higher binding capacity than that of the MWNTs@NIPs. It can be attributed that the MWNTs@NIPs had not generated specific recognition sites due to the absence of oleanolic acid during the preparation process. Because of the functional groups were randomly arranged in the polymerization process, the MWNTs@NIPs could combine less oleanolic acid molecules. Hence the imprinting effect of MWNTs@NIPs towards oleanolic acid was poorer than that of MWNTs@MIPs.

The dependence of the initial concentration on the adsorbed amount of oleanolic acid on the MWNTs@MIPs or MWNTs@NIPs was investigated and the results were shown in Fig. S3a. The results showed that with increasing initial concentration of oleanolic acid, the maximum adsorption amount was achieved at the concentration of 50 mg L^{-1}, which represented that the adsorption of the specific sites on the MWNTs@MIPs was saturated. MWNTs@NIPs exhibited the same trend as MWNTs@MIPs with a lower saturated adsorption amount.

Based on Langmuir adsorption equation, the values of Langmuir adsorption equilibrium constant K and the saturated adsorption capacity Q_{max} can be calculated by plotting C_e/Q versus C_e. From the equation of $y=0.0323x+0.1318$ ($R^2=0.991$) (shown in Fig. S3b), the values of Q_{max} and K for the MWNTs@MIPs were calculated as 30.96 mg g^{-1} and 0.24 L mg^{-1}, respectively.

3.4. The selectivity of MWNTs@MIPs

To test the selectivity of the MWNTs@MIPs, besides the template oleanolic acid, three other structurally similar compounds (ursolic acid, rhein and emodin) were selected as interfering substrates. Fig. S4 (shown in Supplementary Material) shows the rebinding capacities of the MWNTs@MIPs and MWNTs@NIPs for the mixture standard solution including oleanolic acid, ursolic acid, rhein and emodin with each concentration of 50 mg L^{-1}. As shown in Fig. S4, the MWNTs@MIPs possessed specific binding to oleanolic acid, and recognition for all adsorbates followed the order oleanolic acid > ursolic acid > rhein > emodin. Although the same hydrogen bond can form between the adsorbates and MWNTs@MIPs, the different recognition effects may be caused by the distinct size, structure and functional groups of the template. Table 1 summarizes the distribution coefficient K_d, selectivity coefficient k and relative selectivity coefficient k' values of the MWNTs@MIPs and MWNTs@NIPs. The relative selectivity coefficient k' is an indicator to express the adsorption affinity of recognition sites to the template oleanolic acid. From Table 1, the values of k' for oleanolic acid, ursolic acid, rhein and emodin were 2.93, 1.42, 1.30 and 1.21, respectively. Obviously, the MWNTs@MIPs exhibited higher imprinting factor and specific rebinding capacity toward oleanolic acid than those toward the other three non-templates compounds. It can be concluded that the MWNTs@MIPs showed a preference for oleanolic acid, which confirmed the selectivity of the MWNTs@MIPs.

Table 1
The distribution coefficient (K_d), selectivity coefficient (k) and relative selectivity coefficient (k') of the MWNTs@MIPs and MWNTs@NIPs.

Sample		Q(mg g^{-1})	K_d (L g^{-1})	k	k'
MWNTs@MIPs	Oleanolic acid	28.9	1.41	–	–
	Ursolic acid	19.9	0.67	2.11	–
	Rhein	18.0	0.57	2.48	–
	Emodin	16.6	0.50	2.81	–
MWNTs@NIPs	Oleanolic acid	16.1	0.48	–	2.93
	Ursolic acid	15.9	0.47	1.02	1.42
	Rhein	15.1	0.44	1.10	1.30
	Emodin	14.5	0.41	1.17	1.21

3.5. Optimization of the MISPE procedures

Before the proposed MISPE column was applied to sample analysis, several parameters, such as the solvent of loading, washing and elution, were investigated. Firstly, loading solvents with different polarities, such as THF, DMF and methanol, were investigated. Ten milliliters of 50 mg L^{-1} oleanolic acid solutions of the three solvents above were loaded onto the MISPE column at a rate of 1.0 mL min^{-1}, respectively. And the rebinding of oleanolic acid was tested. As shown in Table 2, oleanolic acid dissolved in methanol had better retention on MISPE column than that in THF and DMF. As MWNTs@MIPs was prepared in DMF, it was anticipated that the best binding would be obtained in this solvent. However, the results showed that the recovery percentage of oleanolic acid retained in MISPE column was less than 80%, which may be due to the good solubility of oleanolic acid in DMF. And it could be explained that solvation of DMF involved intermolecular interactions of the same nature as monomer-template, so DMF acted as a competitor of oleanolic acid [28]. Thus methanol was selected as the optimized loading solution.

The washing step was the most crucial procedure to decrease non-specific interactions, discard matrix components in the

Table 2
Recovery percentages of oleanolic acid obtained from MWNTs@MIPs-SPE and MWNTs@NIPs-SPE under different loading, washing and eluting solutions.

Item	Content	Recovery percentages (%) $n=3$	
		MWNTs@MIPs	MWNTs@NIPs
Loading solutions (10 mL 50 mgL^{-1})	Tetrahydrofuran	16.3 ± 3.5	19.4 ± 2.6
	N, *N*-dimethylformamide	34.7 ± 3.4	21.9 ± 4.2
	Methanol	9.4 ± 1.9	15.2 ± 3.7
Washing solutions (3 mL)	Chloroform	10.9 ± 2.9	11.6 ± 3.2
	Acetonitrile	6.7 ± 1.8	17.4 ± 1.8
	Methanol	14.5 ± 4.3	16.1 ± 2.7
Elution solutions(fractions of acetic acid in methanol)	1%	53.7 ± 2.1	36.9 ± 1.8
	3%	65.4 ± 2.4	40.3 ± 2.3
	5%	78.3 ± 3.1	43.6 ± 2.5
	8%	89.1 ± 4.7	52.8 ± 3.8
	10%	90.2 ± 3.4	56.3 ± 4.1
	12%	89.9 ± 2.9	56.8 ± 2.7
	15%	89.5 ± 3.4	55.9 ± 3.2
	18%	89.0 ± 3.2	56.1 ± 2.6
	20%	89.2 ± 3.6	56.8 ± 2.9

polymer and simultaneously maximize the specific interactions between the template and binding sites [29]. During the washing process, interferences and oleanolic acid bound non-specifically to the imprinted polymer would be eluted, while most of oleanolic acid bound specifically remained in the polymers matrix due to the specific interactions. Washing step was conducted with chloroform, acetonitrile and methanol, respectively. As shown in Table 2, the MISPE column washed with acetonitrile had the lowest recovery percentage of 6.7%, while that of the non-imprinted SPE (NISPE) column was 17.4%. It was demonstrated that acetonitrile could effectively remove the interfering compounds from samples to reduce the matrix effect. In contrast, the recovery percentages obtained from chloroform and methanol were 14.5% and 10.9% from MISPE column, respectively. It was found that chloroform and methanol were sufficient to remove interferences, but most of oleanolic acid was also eluted from the MISPE column. Considering recovery percentages, purification efficiency, it could be concluded that acetonitrile was the most effective washing solvent, which could remove interferences efficiently and retain the most of oleanolic acid specifically bound from the MISPE column.

To enhance the specific extraction process of oleanolic acid, the elution solution composed of acetic acid and methanol was optimized. Ten milliliters of methanol containing 1–20% acetic acid solution were percolated through the MISPE and NISPE columns, respectively. As shown in Table 2, with increased acetic acid in methanol, the recoveries of oleanolic acid eluted increased in the range of 1–10% but no obvious increasing from 12% to 20%, which indicated that methanol solution involving 10% acetic acid could elute effectively most of oleanolic acid from the MISPE column. It can be attributed that the acidic conditions could disrupt the electrostatic interactions, hydrogen bond and ionic interaction between oleanolic acid and the functional groups, thus improve the recovery percentage of the template oleanolic acid. And the interactions of oleanolic acid and MWNTs@MIPs were mainly via hydrogen bond and ionic interaction of amino groups and the phenyl groups on the MWNTs@MIPs. Meanwhile oleanolic acid could be retained on the MWNTs@MIPs by hydrophobic forces. Thus, 10 mL of 10% acetic acid solution was employed as the eluting solution to strip oleanolic acid from the MISPE column.

The optimal MISPE protocol was loading with methanol, washing with 3 mL acetonitrile, and eluting with 3 mL 10% acetic acid solution.

3.6. Application

To demonstrate the ability of MIPs to extract oleanolic acid from real samples, oleanolic acid in the roots of kiwi fruit samples was separated and determined under the optimized conditions by coupling MISPE and HPLC. Fig. 5 illustrates the chromatograms of the roots of kiwi fruit samples before or after treated by the MISPE column. The chromatograms showed that oleanolic acid was extracted effectively with MISPE (shown in Fig. 5b). And chromatogram of eluting solutions was shown in Fig. 5c, in which oleanolic acid was remarkably concentrated. According to chromatograms in Fig. 5, the MISPE exhibited excellent selectivity and enrichment ability towards oleanolic acid due to special imprinted cavities that were complementary in size, shape, and functionality ready for oleanolic acid recognition. And the concentration of oleanolic acid in the roots of kiwi fruit extracts was calculated as 0.21 mg L^{-1}. The linear range was 10–60 mg L^{-1} with a limit of detection (LOD) based on the signal-to-noise ratio of 2.56 μg L^{-1} ($R^2=0.994$). The precision of the method was evaluated by calculating the relative standard deviation (RSD) of the extraction at the three different concentration levels using the optimized procedures. The results were shown in Table 3. When 1.0, 2.0 and 3.0 mg L^{-1} of oleanolic acid, ursolic acid, rhein and emodin were added, satisfactory recoveries of oleanolic acid were found to be in the range of 84.0–92.6% for the three kiwi fruit samples, with relative standard deviations of 3.2∼4.5%. And the recoveries of ursolic acid, rhein and emodin were 55.0–60.7%, 48.0–47.7% and 51.0–60.7%, respectively. These results confirmed the potential applicability of the MWNTs@MIPs prepared in the present work for effective pre-concentration, separation and accurate determination of oleanolic acid in real samples.

4. Conclusions

An oleanolic acid imprinted polymer was synthesized successfully using 4-vinyl pyridine and divinylbenzene as the functional monomer and cross linker, respectively. The synthesized imprinted polymer showed specific binding of oleanolic acid. The values of Langmuir adsorption equilibrium constant K and theoretical maximum adsorption capacity Q_{max} were caculated to be 0.24 L mg^{-1} and 30.96 mg L^{-1}, respectively. The MWNTs@MIPs were

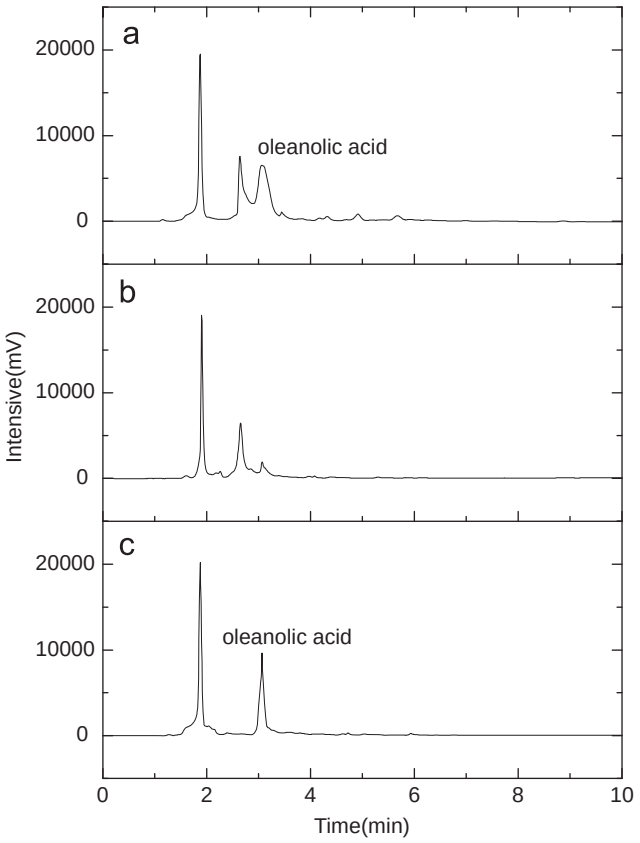

Fig. 5. (a) Chromatogram of crude extract of roots of kiwi fruit samples, (b) chromatogram of crude extract of roots of kiwi fruit samples with MWNTs@MIPs, and (c) chromatogram of eluting solutions from MWNTs@MIPs/SPE column of crude extract of kiwi fruit roots.

Table 3
Recoveries at different spiked levels of oleanolic acid, ursolic acid, rhein and emodin in kiwi fruit samples.

Sample	Spiked level ($mg\,L^{-1}$)	Found ($mg\,L^{-1}$)	Recoveries [a] (%)	RSD [b] (%) ($n=3$)
Oleanolic acid	1.00	0.84	84.0	3.2
	2.00	1.81	90.5	4.0
	3.00	2.78	92.6	4.5
Ursolic acid	1.00	0.55	55.0	2.4
	2.00	1.23	61.5	3.1
	3.00	1.97	65.7	3.8
Rhein	1.00	0.48	48.0	2.6
	2.00	1.06	53.0	3.3
	3.00	1.73	57.7	3.6
Emodin	1.00	0.51	51.0	2.9
	2.00	1.09	54.5	3.4
	3.00	1.82	60.7	3.7

[a] Recovery $\%=(C_{\text{spike sample}}-C_{\text{non-spike sample}})/C_{\text{added}}\times 100\%$, where $C_{\text{spike sample}}$ and $C_{\text{non-spike sample}}$ represent the concentration of the analyte in spiked samples and non-spiked samples, respectively, C_{added} is the concentration of the analyte added.

[b] RSD is the relative standard deviation.

successfully used as SPE materials to selectively enrich and determine oleanolic acid from the roots of kiwi fruit samples combined with HPLC. The proposed method provides an effective tool for enriching and detecting oleanolic acid in many complicated matrices.

Acknowledgment

This work is supported by the National Natural Science Foundation of China (No. 21005030), the Research Foundation of Education Bureau of Hunan Province, China (No.10A099), the 12th Five-year-plan National Technology Support Program, China (No. 2011BAD10B01) and Science and Technology Innovative Research Team in Higher Educational Institutions of Hunan Province.

Appendix A. Supporting information

Supplementary data associated with this article can be found in the online version at http://dx.doi.org/10.1016/j.talanta.2012.07.066.

References

[1] L.O. Somova, A. Nadar, P. Rammanan, F.O. Shode, Phytomedicine 10 (2003) 115–121.
[2] I. Sogno, N. Vannini, G. Lorusso, R. Cammarota, D.M. Noonan, A. Albini, Recent Results Cancer Res. 181 (2009) 209–212.
[3] J. Pollier, A. Goossens, Phytochemistry 77 (2012) 10–15.
[4] E.Q. Xia, Y.Y. Yu, X.R. Xu, G.F. Deng, Y.J. Guo, H.B. Li, Ultrason. Sonochem. 19 (2012) 772–776.
[5] R. Zhu, W.H. Zhao, M.J. Zhai, F.D. Wei, Z. Cai, N. Sheng, Q. Hu, Anal. Chim. Acta 658 (2010) 209–216.
[6] S.L. Zhang, Z. Du, G.K. Li, Anal. Chem. 83 (2011) 7531–7541.
[7] S. Iman, M.R. Hadjmohammadi, P. Moazameh, I. Mehrdad, B. Behruz, A.B. Babaei, A.M. Dust, J. Pharm. Biomed. Anal. 56 (2011) 419–422.
[8] B. Sellergren, Anal. Chem. 66 (1994) 1578–1582.
[9] S. Ambrosini, M. Serra, S. Shinde, J. Chromatogr. A 1218 (2011) 6961–6969.
[10] Q.Q. Gai, F. Qu, Z.J. Liu, R.J. Dai, Y.K. Zhang, J. Chromatogr. A 1217 (2010) 5035–5042.
[11] Y. Umasankar, T.Y. Huang, S.M. Chen, Anal. Biochem. 408 (2011) 297–303.
[12] N. Kirsch, J. Hedin-Dahlström, H. Henschel, M.J. Whitcombe, S. Wikman, I.A. Nicholls, J. Mol. Catal. B: Enzyme 58 (2009) 110–117.
[13] Y.T. Liu, R.H. Liu, C.B. Liu, S.L. Luo, L.X. Yang, F. Sui, Y.R. Teng, R.B Yang, Q.Y. Cai, J. Hazard. Mater. 182 (2010) 912–918.
[14] M. Karabork, A. Ersoz, A. Denizli, R. Say, Ind. Eng. Chem. Res. 47 (2008) 2258–2264.
[15] T.Y. Li, S.X. Chen, H.C. Li, Q.H Li, L. Wu, Langmuir 27 (2011) 6753–6758.
[16] J.D. Ryckman, M. Liscidini, J.E. Sipe, S.M. Weiss, Nano Lett. 11 (2011) 1857–1862.
[17] J.M. Pan, H. Yao, L.C. Xu, H.X. Ou, P.W. Huo, X.X. Li, Y.S. Yan, J. Phys. Chem. C 115 (2011) 5440–5449.
[18] P.S. Lee, X.Y. Zhang, J.A. Stoeger, A. Malek, W. Fan, S. Kumar, W.C. Yoo, S.A. Hashimi, R.L. Penn, A. Stein, M. Tsapatsis, J. Am. Chem. Soc. 133 (2011) 493–502.
[19] J.M. Gong, X.J. Miao, T. Zhou, L.Z. Zhang, Talanta 85 (2011) 1344–1349.
[20] M.S Zhang, J.R. Huang, P. Yu, X. Chen, Talanta 81 (2010) 162–166.
[21] A. Hirano, K. Uda, Y. Maeda, T. Akasaka, K. Shiraki, Langmuir 26 (2010) 17256–17259.
[22] Z.K. Lin, W.J. Cheng, Y.Y. Li, Z.R. Liu, X.P. Chen, C.J. Huang, Anal. Chim. Acta 720 (2012) 71–76.
[23] M. Karabork, A. Ersoz, A. Denizli, R. Say, Ind. Eng. Chem. Res. 47 (2008) 2258–2264.
[24] V. Thibert, P. Legeay, F. Chapuis-Hugon, V. Pichon, Talanta 88 (2012) 412–419.
[25] H. Zeng, Y.Z. Wang, X.J. Liu, J.H. Kong, C. Nie, Talanta 93 (2012) 172–181.
[26] Á. Valero-Navarro, M. Gómez-Romero, J.F. Fernández-Sánchez, P.A. Cormack, A. Segura-Carretero, A. Fernández-Gutiérrez, J. Chromatogr. A 1218 (2011) 7289–7296.
[27] X.Z. Shi, A.B. Wu, S.L. Zheng, R.X. Li, D.B. Zhang, J. Chromatogr. B 850 (2007) 24–30.
[28] M.B. Gholivand, M. Torkashvand, G. Malekzadeh, Anal. Chim. Acta 713 (2012) 36–44.
[29] D.K. Alexiadou, N.C. Maragou, N.S. Thomaidis, G.A. Theodoridis, M.A. Koupparis, J. Sep. Sci. 31 (2008) 2272–2282.